Nanoparticulate Cellular Patches for Cell-Mediated Tumoritropic Delivery

Hao Cheng,[†,‡] Christian J. Kastrup,[†] Renuka Ramanathan,[§] Daniel J. Siegwart,[†] Minglin Ma,[†,∥] Said R. Bogatyrev,[‡] Qiaobing Xu,[†,‡] Kathryn A. Whitehead,[†] Robert Langer,[†,‡] and Daniel G. Anderson[†,*]

[†]The David H. Koch Institute for Integrative Cancer Research, [‡]Department of Chemical Engineering, [§]and Department of Biological Engineering, Massachusetts Institute of Technology, 77 Massachusetts Avenue, Cambridge, Massachusetts 02139, and [∥]Children's Hospital Boston, 300 Longwood Avenue, Boston, Massachusetts 02115

ABSTRACT The targeted delivery of therapeutics to tumors remains an important challenge in cancer nanomedicine. Attaching nanoparticles to cells that have tumoritropic migratory properties is a promising modality to address this challenge. Here we describe a technique to create nanoparticulate cellular patches that remain attached to the membrane of cells for up to 2 days. NeutrAvidin-coated nanoparticles were anchored on cells possessing biotinylated plasma membrane. Human bone marrow derived mesenchymal stem cells with nanoparticulate patches retained their inherent tumoritropic properties as shown using a tumor model in a 3D extracellular matrix. Additionally, human umbilical vein endothelial cells with nanoparticulate patches were able to retain their functional properties and form multicellular structures as rapidly as unmodified endothelial cells. These results provide a novel strategy to actively deliver nanostructures and therapeutics to tumors utilizing stem cells as carriers and also suggest that nanoparticulate cellular patches may have applications in tissue regeneration.

KEYWORDS: lipid raft · drug delivery · tissue engineering · endocytosis · membrane curvature · cell therapy

Nanostructures have emerged as promising modalities to deliver therapeutics for many applications.[1−4] These nanovehicles offer a number of potential advantages for therapeutic delivery including the ability to protect and controllably release therapeutic molecules, as well as alter their pharmacokinetic properties and biodistribution. Nanostructures have also shown utility in cancer therapy, as in some instances they can be passively targeted to tumors due to the leaky character of tumor vasculature.[5] However, significant barriers to tumor targeting remain, including the potential rapid clearance of nanostructures by liver, kidney, and the immune system. Many strategies have been investigated to reduce the clearance of nanostructures and enhance the therapeutic delivery to tumors, including variations in the size,[6,7] shape,[8,9] flexibility,[8] and surface properties.[10,11] Modifying the surface of nanostructures with ligands that bind specific cancer receptors has been reported to improve their targeting to cancer cells.[12−14]

In some systems, stem cells have been demonstrated to possess tumoritropic properties, and this inherent migratory property has been utilized in the study for potential utility in cancer therapies.[15,16] Although the role of stem cells in tumors remains debated,[17,18] stem cells genetically engineered to produce antitumor proteins have been reported to have efficacy in a number of *in vivo* cancer models, including brain and disseminated tumors.[19,20] We hypothesized that stem cells modified to carry nanoparticulate payloads could be developed to allow for stem-cell-mediated delivery of synthetic, nanoparticulate cancer therapeutics. This strategy contrasts with current stem-cell-based tumoritropic therapies, which are based on the genetic modification of stem cells.[15]

Active delivery of nanoparticles to the center of tumor spheroids by cells has previously been reported using macrophages.[21] In that system, macrophages delivered internalized Au nanoparticles to tumor spheroids, which were then destroyed by irradiation with near-infrared light.[21] Although delivery of particles that have been internalized by cells may prove useful for some applications, delivery of nanostructures external to the stem cell may allow for more effective delivery of drug payloads and reduce the influence and toxicity of therapeutics on the carrier cells. Recently, Swiston and co-workers reported the attachment of micrometer scale polymer layers to the cell membrane, creating cellular patches.[22] The migration of patch-modified T cells on substrates coated with adhesion ligands suggested the potential biomedical applications of this technique. However,
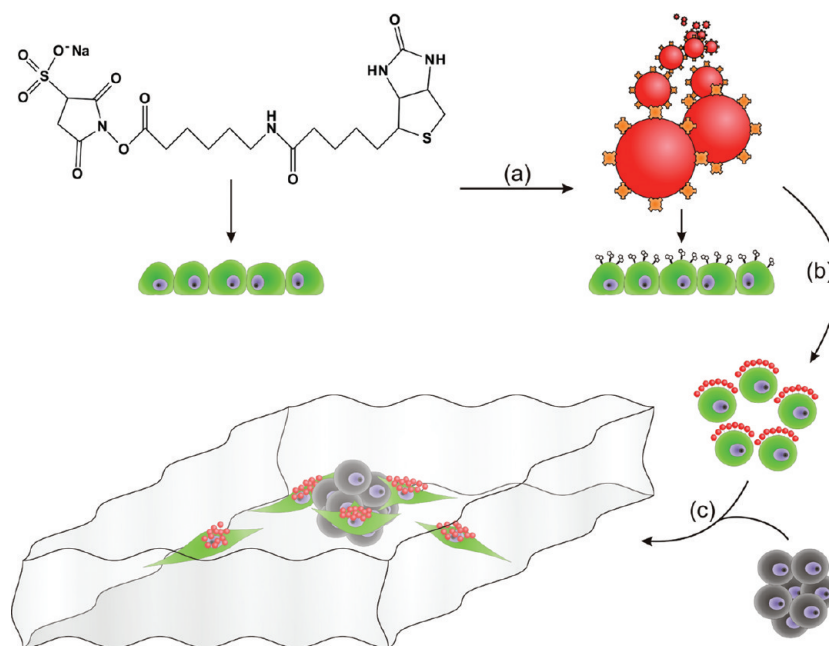
Figure 1. Schematic illustration of stem-cell-mediated delivery of nanoparticles to tumor spheroids in an *in vitro* tumor model. (a) Surface of hMSCs (green) is modified to present biotin. (b) Nanoparticles (red) presenting NeutrAvidin (orange) are anchored to the biotinylated hMSCs. (c) In the presence of a tumor spheroid (gray), the modified hMSCs migrate toward the spheroid and deliver nanoparticles to it.

the relatively large size of the reported patches (10 μm) may limit cellular function.

Nanoparticles attached on red blood cells (ghost cells) were demonstrated to have longer half-life during circulation.[23] However, nanoparticles have a tendency to be internalized when near cellular membranes of regular cells, and this is one of the obstacles to creating durable cell membrane anchors.[24] This may be particularly challenging with tumoritropic cells migrating in extracellular matrix (ECM) as migrating cells have been reported to have increased internalization activity.[25]

Herein, we report a strategy to create nanoparticulate patches on the membrane of cells. These nanoparticulate patches remain on the membrane of cells for days and may provide a method to deliver nanotherapeutics using cells.

RESULTS AND DISCUSSION

Anchoring Nanoparticles on Cell Membranes. Nanoparticulate cellular patches were conjugated to the cellular

membrane as follows. First, the cellular membrane was modified to include biotin. Since primary amines are common active moieties on cell membranes, we biotinylated cell membranes by reacting sulfosuccinimidyl-6-(biotinamido)hexanoate (Sulfo-NHS-LC-Biotin) with cell membrane amines. The conjugation of biotins to the cell membrane provided the binding sites to which NeutrAvidin-coated nanoparticles could anchor (Figure 1). To confirm that the cell membrane was modified with biotin, cells were probed with Alexa 488 streptavidin and imaged by fluorescent microscopy (Figure 2). HeLa cells were first treated with Sulfo-NHS-LC-Biotin at various concentrations (2, 0.67, 0.2, and 0.067 mM) and were then incubated with Alexa 488 streptavidin. After fixation, cells were imaged with a laser scanning confocal microscope. Fluorescence intensity increased with Sulfo-NHS-LC-Biotin concentration, indicating the presence of membrane-bound biotin.

Next, NeutrAvidin-modified nanoparticles were allowed to react with biotinylated cells. We tested the conjugation of nanoparticles with both biotinylated hu-
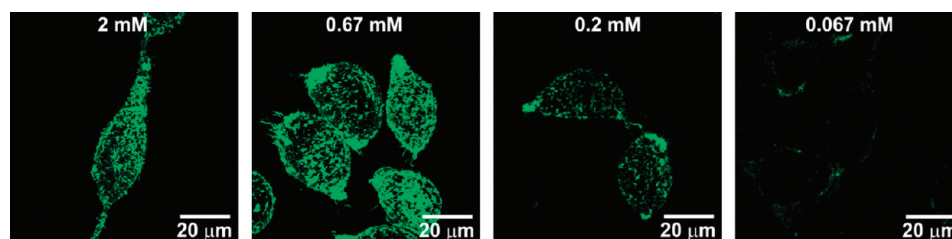

Figure 2. Fluorescence of Alexa 488 streptavidin probe on biotinylated cells. Cells were pretreated with various concentrations of Sulfo-NHS-LC-Biotin, while the concentration of the steptavidin probe remained constant. The confocal images were obtained by focusing on the top of the cell membranes, except for the 0.067 mM condition where the microscope was focused on the bottom of cells due to weak signal at the top of cell membranes.
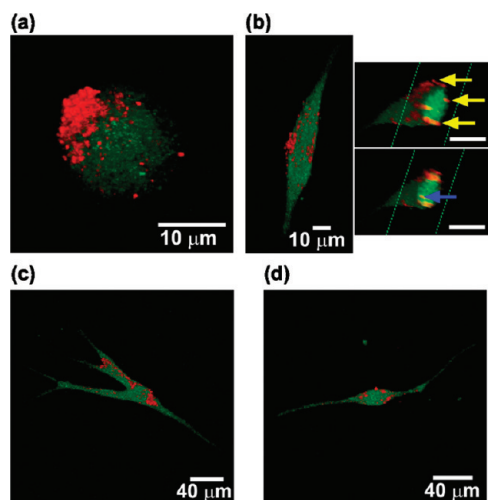
Figure 3. Three-dimensional reconstructed confocal microscopy images of hMSCs (green, cell tracker dye) coated with nanoparticles (red) in a 3D collagen I gel. (a) A representative modified hMSC after detachment from its substrate by trypsinization. (b) hMSC within the collagen gel grown for 2 days. Two cross-sectional views (insets) show nanoparticles internalized within the cell (blue arrow) and on the surface of the cell membrane (yellow arrows). (c,d) hMSCs within the collagen gel have nanoparticle associated primarily on the main cell body rather than on the long cell protrusions.
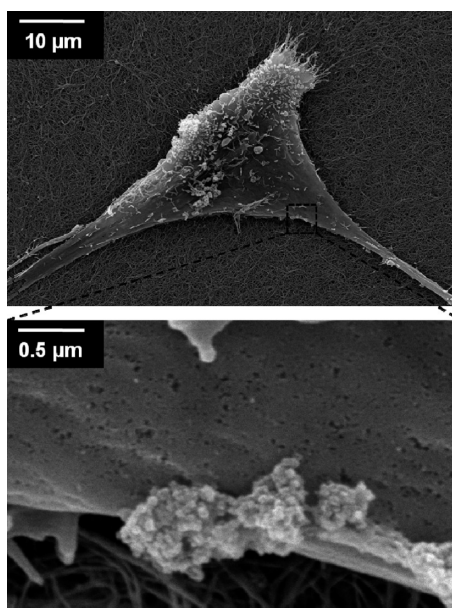

Figure 4. Scanning electron microscopy images of nanoparticle clusters on a hMSC cell membrane. A hMSC grew for 2 days on collagen I gel after nanoparticles were anchored.

man bone marrow derived mesenchymal stem cells (hMSCs) and human umbilical vein endothelial cells (HUVECs). Cells were fluorescently labeled by incubating them with a fluorescent cell-tracker dye, 5-chloromethylfluorescein diacetate. A model nanoparticle was used—monodisperse NeutrAvidin-coated 40 nm polystyrene nanoparticles that fluoresced at 605 nm. The size of the nanoparticles was confirmed using scanning electron microscopy (SEM) (Supporting Information Figure S1). When incubated with cells, nanoparticles attached only on the portion of membrane exposed to reagents in the media, as Sulfo-NHS-LC-Biotin and nanoparticles are not cell membrane permeable. Initially, this created an asymmetric distribution of nanoparticulate cellular patches on the cells. Although loosely bound particles were rinsed away, some particles remained on cells through nonspecific interactions rather than the specific biotin−NeutrAvidin binding in our experimental condition (Figure S2). Bovine serum albumin (BSA) or other blocking solutions can be used in the step of nanoparticle attachment on cell membrane to block or reduce the nonspecific binding of the nanoparticles. However, these solutions were not used here so that the highest possible loading of particles onto the cells would be achieved.

Characterization of Nanoparticulate Cellular Patches. To confirm that nanoparticles were attached to biotin-modified hMSCs, we used confocal microscopy. The results demonstrated that nanoparticulate patches formed on the surface of cells (Figure 3). The asymmetric distribution of nanoparticles could be observed at early time points in 3D reconstructed confocal images (Figure 3a). The hMSCs were then seeded in 1 mg/mL

collagen I gels, which mimics some aspects of the *in vivo* microenvironment. Cells were imaged after 2 days in 3D gels to determine whether nanoparticles were internalized. Although internalized nanoparticles were observed, there were also substantial amounts of nanoparticles localized on the membranes of cells as seen in 3D reconstructed images (Figure 3b). Interestingly, most of the membrane-associated nanoparticles localized on the main body of hMSCs, and nanoparticles were rarely observed on the dendrite-like long protrusions of the cells (Figure 3c,d). This phenomenon was always observed for hMSCs in a wide range of morphologies. These long protrusions are related to cell migration and undergo rapid membrane reorganization.[26,27] It is possible that nanoparticles on the cell membrane may affect the membrane reorganization by interacting with receptors. It remains to be determined whether cells passively protrude areas of their membrane where fewer nanoparticles are anchored, or if cells can reorganize their membrane and shift nanoparticles to positions on the membrane that are less critical for cell mobility.

To further confirm that nanoparticles were anchored on the outer cell membrane and investigate the morphology of the cellular patches, we imaged the modified cells using SEM. hMSCs coated with anchored nanoparticles were cultured on top of collagen I gels (1 mg/mL) for 2 days, then fixed and dried for SEM analysis. These SEM images show that the nanoparticles normally exist as clusters on the cell membrane (Figure 4). For example, in one portion of the cell in Figure 4, there are three nanoparticle clusters located on the cell membrane, with cluster sizes of 400 × 400, 500 × 650, and 700 × 850 nm. The clustering of nanoparti-

cles on the membrane may be due to membrane reorganization of the particles. The binding of small-sized nanostructures on cells causes cell membrane curvature, which increases the elastic energy of the membrane. Small nanostructures on cell membranes are known to form clusters at a size sufficient to lower the elastic energy and to allow the membrane to wrap around the particles for endocytosis.[28,29] Although the formation of large clusters of nanostructures may result from movement of nanoparticles at the surface of the membrane, an alternative explanation is that the nanoparticles aggregated in solution prior to binding to the cell membrane.

To test if the second explanation is occurring, phase analysis light scattering was used to determine the particle size distribution in solution. The concentration of particles in solution was the same as the concentration of particles used during attachment to cells. Particle volume counting was used to characterize the fraction of aggregated nanoparticles. The light scattering results showed that $86.5 \pm 2\%$ of the nanoparticles were monodisperse, with a diameter of ~40 nm, and $13.5 \pm 2\%$ of the nanoparticles were aggregated in solution, with the size of the aggregates ranging from 150 to 250 nm (Supporting Information Figure S3). Although some aggregation of nanoparticles was seen in solution, these aggregates had a volume of several times smaller than the clusters of nanoparticles observed on the cell membrane, indicating that aggregation in solution alone cannot explain the clusters seen on the cell membrane. Additionally, we observed some clustering of nanoparticles over time on the surface of cells using fluorescence microscopy (Supporting Information, Figure S4). It is possible that clusters of particles are internalized slower than individual particles. We hypothesize that the internalization and clustering may be kinetically competing process—if internalization is slower than movement of particles on the surface and clustering, then large clusters will form eventually, reducing the rate of internalization. The small portion of aggregated nanoparticles seen in solution may indicate some extent of hydrophobic interactions between nanoparticles, and this may also have contributed to the clustering of nanoparticles seen on cell membranes.

Response of Tumoritropic Stem Cells with Nanoparticulate Patches to Tumor Spheroids. hMSCs are widely used tumoritropic stem cells in *in vivo* tumor models.[15,30] To determine whether hMSCs maintain their intrinsic capacity to sense tumors after nanoparticles are anchored on the surface, we used an *in vitro* tumor model consisting of a tumor spheroid grown in an ECM. The precise mechanism of how hMSCs track tumors is not fully understood, but several mechanisms may be important. It has been suggested that cancer cells induce the surrounding vasculature to express adhesion molecules which tether circulating hMSCs and result in cell rolling, and it has also been suggested that hMSCs can sense the

gradient of tumor relevant chemokines and growth factors, such as stromal-cell-derived factor 1 (SDF-1) and platelet-derived growth factor (PDGF).[31−33] We grew liver tumor spheroids composed of mouse embryonic fibroblasts (MEFs), HUVECs, and human liver cancer cells (Hep G2). Each tumor spheroid was cocultured in collagen I gel with either hMSCs with nanoparticles anchored on them or hMSCs without nanoparticles. The substrates were pretreated with agarose gel to prevent the collapse of the tumor spheroid due to adhesion of cells to the substrate. Both groups of hMSCs, with and without nanoparticulate cellular patches, sensed and responded to tumor spheroids rapidly as indicated by the cells polarizing themselves in line with the spheroid within 12 h (Figure 5a,b). The degree of polarization of each cell was characterized by measuring the angle between the long axis of the cell and the vector connecting the center of the cell and the center of the spheroid. Theoretically, a sample of cells that did not polarize toward the spheroid would have an average angle of 45°, whereas a sample of cells that perfectly polarized would have an average angle of 0°. In an experimental control sample without a spheroid, the average angle of hMSCs was 42°. In contrast, a sample containing a spheroid and hMSCs anchored with nanoparticles had a significantly lower average angle of 20° ($P < 0.001$). There was no significant difference between hMSCs with or without nanoparticles ($P > 0.1$), where the hMSCs without particles had an average angle of 27°. Therefore, we demonstrated that stem cells anchored with nanoparticulate patches retain their ability to sense tumor spheroids, which suggests that they may be used as a strategy to deliver nanostructures to tumors.

Formation of Tubular-like Structures by Endothelial Cells Modified with Nanoparticulate Cellular Patches. In addition to active delivery of nanoparticles to tumors, the technique of anchoring nanoparticles on cell membranes may have other biomedical applications. For example, we hypothesize that surface-bound nanoparticles may be used in tissue regeneration to stimulate functions of the cells they are attached to or to regulate cell−cell communication through the controlled release of therapeutics. A prerequisite of these applications is that the cellular patch itself should not negatively affect the intrinsic function of the tissue regenerating cells, such as inhibiting their ability to form multicellular structures. To test if anchoring nanoparticles to cells would inhibit this ability, we attached nanoparticles on the membrane of HUVECs and monitored the formation of tubular-like structures on Matrigel. HUVECs are well-known to rapidly form tubular-like structures on gels due to their intrinsic ability to construct vessels. Both untreated HUVECs and HUVECs with nanoparticulate patches initiated the formation of tubular-like structures when grown on Matrigel for 4 h (Supporting Information Figure S5). The ability of cells associated with
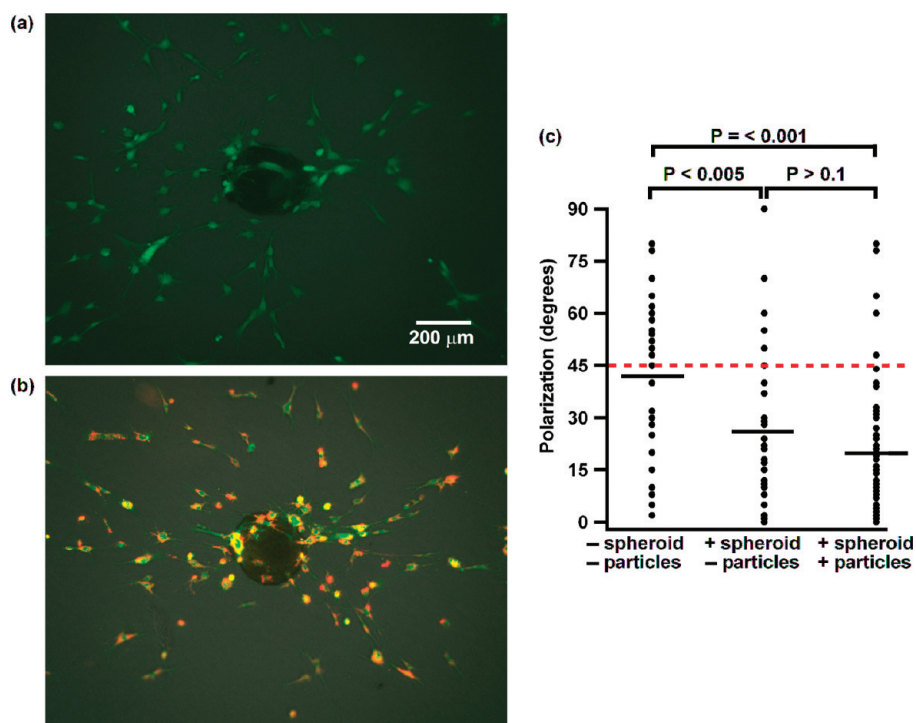
Figure 5. hMSCs respond and polarize to tumor spheroids in collagen gel. (a) Fluorescence image of a control experiment of hMSCs without nanoparticles (green) and a tumor spheroid (overlaid phase-contrast image). (b) Image of hMSCs coated with nanoparticles (red) and a tumor spheroid. (c) Graph quantifying the amount of polarization. Each data point indicates the angle between the long axis of a single cell and the vector connecting the center of the cell with the center of the spheroid. *P* values are given for each data set. The red dashed line indicates the theoretical average degree for a set of cells that are not polarized. The short black lines indicate the average degree of each data set.

nanoparticles to rapidly spread and move on the ECM is likely due to the initial asymmetric coverage of particles on the membrane as a majority of cell membrane was not affected by nanoparticles. The tubular-like structure of HUVECs coated with nanoparticles was analyzed by confocal microscopy after 24 h. All HUVECs participated in the formation of tubular-like structures on the gel, and no particles were observed to be shed by cells (Figure 6a). A high-magnification confocal image (Figure 6b) and a 3D reconstructed image (Figure 6c) show that most of the nanoparticles were localized on the cell membrane and had not been endocytosed by cells. These results demonstrate that when nanoparticles are anchored on the membrane of HUVECs they do not affect the formation and rate of formation of tubular-like structures.

CONCLUSION

In conclusion, we have anchored nanoparticles on the membrane of cells and demonstrated that this process does not affect the intrinsic cell functions evaluated here. hMSCs attached with nanoparticles do not lose their capacity to sense and respond to tumor spheroids grown in 3D collagen gels, and HUVECs associated with nanoparticles can still form tubular-like structures on Matrigel. Previous reports indicate that nanostructures bound on cells are typically internalized easily on the time scale of minutes or hours,[24]

whereas the accumulation of hMSCs in tumors occurs on the time scale of days.[16,30,34] The results here show that a substantial amount of nanoparticles can be kept on the surface of cells for a longer period of up to 2 days. We hypothesize that the reduced rate of internalization of nanoparticles into cells may be a consequence of the nanoparticulate patches binding to a
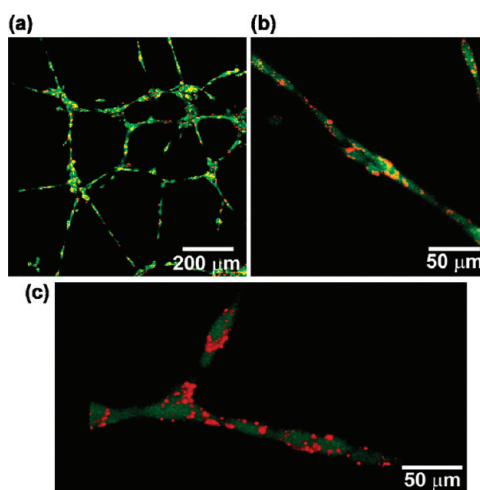

Figure 6. HUVECs coated with 40 nm nanoparticles form tubular-like structures on Matrigel. Confocal microscopy images were taken of HUVECs (green) coated with nanoparticles (red) after 24 h of growth. (a) Network of HUVECs. (b) Higher magnification image. (c) Three-dimensional reconstructed confocal image of HUVECs coated with nanoparticles.

ARTICLE

large number of transmembrane proteins simultaneously. The mechanism of cell endocytosis requires the cooperation among several proteins and involves protein conformation changes.[35] By binding to a large number of biotin-modified proteins, it may be that the nanoparticulate patches disrupt this cooperation and reduce endocytosis. The eventual formation of relative large-sized patches (several hundred nanometers) may also be important for the slow endocytosis.

We believe that nanoparticulate cellular patches may prove to be useful tools for cell-based therapies such as tissue regeneration and tumoritropic cell-mediated delivery of nanoparticles to tumors. Specifically, these techniques may provide methods to allow for stem-cell-mediated delivery of therapeutic agents without the need for viral infection. We envision that fabricating nanostructures that bind directly to specific domains of cell surface proteins could further reduce the amount of internalization of nanoparticles. We also envision that the potential of this nanoparticle/cell system for cancer therapy may be improved by designing nanoparticles that assist the stem cells in homing to tumors. For example, particles that bind both stem cells and receptors on the vessel wall near tumors could facilitate targeting. We hypothesize that the transient, external modification of stem cells with ligands and drugs could prove useful in controlling stem cell behavior *in vivo*.

MATERIALS AND METHODS

Materials. Sulfosuccinimidyl-6-(biotinamido)hexanoate (Sulfo-NHS-LC-Biotin) was purchased from Pierce Protein Research Products. NeutrAvidin-labeled 40 nm fluoSphere, CellTracker Green CMFDA (5-chloromethylfluorescein diacetate), UltraPure agarose, fetal bovine serum (FBS), DMEM medium, penicillin and streptomycin, trypsin EDTA, and Alexa 488 streptavidin were purchased from Invitrogen. Rat tail collagen I and Matrigel were purchased from BD Biosciences. Endothelial cell growth medium 2 and mesenchymal stem cell growth medium were purchased from Lonza. Formaldehyde solution (36.5%) and hexamethyldisilazane were purchased from Sigma-Aldrich. Glutaldehyde (10%) was purchased from Electron Microscopy Science.

Cell Culture. Human liver cancer cell line Hep G2 was obtained from ATCC. Mouse embryonic fibroblasts (MEFs) were purchased from Globalstem. Hep G2 and MEF cells were grown at 37 °C/5% CO_2 in DMEM high glucose media supplemented with 10% fetal bovine serum and 100 IU/mL penicillin/streptomycin. Human umbilical vein endothelial cells (HUVECs) and human mesenchymal stem cells (hMSCs) were obtained from Lonza. HUVECs were cultured at 37 °C/5% CO_2 in endothelial cell growth medium 2. hMSCs were cultured at 37 °C/5% CO_2 in mesenchymal stem cell growth medium.

Cell Labeling. Cells were washed three times with DMEM and incubated in 5 μM CMFDA in DMEM at 37 °C/5% CO_2 for 25 min. Following incubation, the CMFDA solution was aspirated and fresh medium was added. Cells were allowed to recover from the treatment for at least 4 h before experiments.

Cell Biotinylation. Cells at 80−90% confluency were washed with PBS three times and were then incubated in a Sulfo-NHS-LC-Biotin PBS solution for 20 min. The Sulfo-NHS-LC-Biotin concentration was 2 mM, unless otherwise specified. Following biotinylation, the cells were washed three times with DMEM high glucose media (without FBS). For probing with Alexa 488 streptavidin, the cells were treated with 15 μg/mL Alexa 488 streptavidin in optiMEM medium on ice for 30 min. Cells were washed and fixed with 4% formaldehyde in PBS for confocal imaging.

Attaching Nanoparticles on Biotinylated Cells. The nanoparticles (NeutrAvidin-labeled 40 nm fluoSpheres) were centrifuged and washed three times with PBS, suspended in 1 mL of DMEM buffer, and sonicated for 2 min to keep nanoparticles in a monodisperse state. The biotinylated cells were treated with 1.5×10^{12} nanoparticles in one well of a 6-well plate for 25 min. Cells were then trypsinized for analysis or used in subsequent experiments.

Scanning Electron Microscopy. Cells coated with nanoparticles were seeded on top of a collagen I gel and were grown for 2 days. To prepare the collagen I gel, a high concentration rat tail collagen I solution was diluted with DMEM medium and neutralized with NaOH solution according to the vendor's protocol to make a final collagen I concentration of 1 mg/mL. The solution was coated on coverslips and incubated at 37 °C for 0.5 h to form the gel. Cells were fixed in 2% formaldehyde and 2% glutalde-hyde PBS solution at room temperature for 20 min. Samples were immersed serially in PBS, ddH₂O, 20% ethanol, 40% ethanol, 60% ethanol, 80% ethanol, and 100% ethanol for 2 min each followed by incubation in hexamethyldisilazane for 20 min. The samples were then allowed to dry in a biosafety hood for 4 h prior to imaging. Samples were sputter-coated with a thin layer of gold using a Hummer 6.2 gold sputtering system (Anatech Ltd.). Scanning electron micrographs were taken using a JEOL JSM-5600LV at 10 kV acceleration voltage.

Measuring the Nanoparticle Size Distribution. Nanoparticles were suspended at a concentration of 1.5×10^{12}/mL in DMEM and sonicated for 2 min and their sizes were measured by light scattering using a ZetaPALS instrument (Brookhaven Instruments Corporation). The concentration of particles in solution was the same as the concentration of particles used during attachment to cells. Particle volume counting was used to characterize the fraction of aggregated nanoparticles. Four samples were measured to obtain a statistical distribution. The result of one sample is shown in Supporting Information Figure S3.

Testing the Response of hMSCs to Tumor Spheroids. The tumor spheroids were grown in a 96-well plate. The plate was initially coated with 1% agarose gel to prevent cell adhesion. Five hundred HUVECs, 500 MEFs, and 600 Hep G2 were seeded in each well to form the spheroid. Cells were grown at 37 °C/5% CO_2 in DMEM high glucose media, supplemented with 10% fetal bovine serum and 100 IU/ml penicillin/streptomycin. Cells aggregated into a single spheroid in each well. After 5 days, spheroids were washed twice with DMEM buffer. Each spheroid and 400 hMSCs were resuspended in 200 μL of 1 mg/mL collagen I DMEM medium. The solution was then transferred to one well of a 48-well plate coated with 1% agarose gel. The plate was kept on ice for 3 min to allow cells to settle to the bottom so that most of the hMSCs would stay in one imaging focal layer. The plate was then incubated at 37 °C/5% CO_2 for 12 h and then imaged.

Formation of HUVEC Tubular-like Structures on Matrigel. To prepare the Matrigel substrate, 80 μL of Matrigel solution was added to the center of a 35 mm coverslip/bottom dish followed by incubation at 37 °C for 20 min; 40 000 HUVECs in 2 mL of medium were then added to the dish. Cells were imaged with a fluorescence microscope (Zeiss Axiovert) after 4 h of growth and with a laser scanning confocal microscope (Zeiss LSM 510) after 24 h of growth.

Calculation of Statistical Significance. Statistical significance was determined by calculating P values using the student's t test (two tailed distribution and two sample unequal variance).

Supporting Information Available: Additional images. This material is available free of charge *via* the Internet at http://pubs.acs.org.

REFERENCES AND NOTES

1. Davis, M. E.; Chen, Z.; Shin, D. M. Nanoparticle Therapeutics: An Emerging Treatment Modality for Cancer. *Nat. Rev. Drug Discovery* **2008**, *7*, 771–782.

2. Peer, D.; Karp, J. M.; Hong, S.; FaroKhzad, O. C.; Margalit, R.; Langer, R. Nanocarriers as an Emerging Platform for Cancer Therapy. *Nat. Nanotechnol.* **2007**, *2*, 751–760.

3. Akinc, A.; Zumbuehl, A.; Goldberg, M.; Leshchiner, E. S.; Busini, V.; Hossain, N.; Bacallado, S. A.; Nguyen, D. N.; Fuller, J.; Alvarez, R.; Borodovsky, A.; Borland, T.; Constien, R.; de Fougerolles, A.; Dorkin, J. R.; Jayaprakash, K. N.; Jayaraman, M.; John, M.; Koteliansky, V.; Manoharan, M.; Nechev, L.; Qin, J.; Racie, T.; Raitcheva, D.; Rajeev, K. G.; Sah, D. W. Y.; Soutschek, J.; Toudjarska, I.; Vornlocher, H. P.; Zimmermann, T. S.; Langer, R.; Anderson, D. G. A Combinatorial Library of Lipid-like Materials for Delivery of RNAi Therapeutics. *Nat. Biotechnol.* **2008**, *26*, 561–569.

4. Wagner, V.; Dullaart, A.; Bock, A. K.; Zweck, A. The Emerging Nanomedicine Landscape. *Nat. Biotechnol.* **2006**, *24*, 1211–1217.

5. Matsumura, Y.; Maeda, H. A New Concept for Macromolecular Therapeutics in Cancer-Chemotherapy—Mechanism of Tumoritropic Accumulation of Proteins and the Antitumor Agent SMANCS. *Cancer Res.* **1986**, *46*, 6387–6392.

6. Yuan, F.; Dellian, M.; Fukumura, D.; Leunig, M.; Berk, D. A.; Torchilin, V. P.; Jain, R. K. Vascular-Permeability in a Human Tumor Xenograft—Molecular-Size Dependence and Cutoff Size. *Cancer Res.* **1995**, *55*, 3752–3756.

7. Kong, G.; Braun, R. D.; Dewhirst, M. W. Hyperthermia Enables Tumor-Specific Nanoparticle Delivery: Effect of Particle Size. *Cancer Res.* **2000**, *60*, 4440–4445.

8. Geng, Y.; Dalhaimer, P.; Cai, S. S.; Tsai, R.; Tewari, M.; Minko, T.; Discher, D. E. Shape Effects of Filaments *versus* Spherical Particles in Flow and Drug Delivery. *Nat. Nanotechnol.* **2007**, *2*, 249–255.

9. Rolland, J. P.; Maynor, B. W.; Euliss, L. E.; Exner, A. E.; Denison, G. M.; DeSimone, J. M. Direct Fabrication and Harvesting of Monodisperse, Shape-Specific Nanobiomaterials. *J. Am. Chem. Soc.* **2005**, *127*, 10096–10100.

10. Owens, D. E.; Peppas, N. A. Opsonization, Biodistribution, and Pharmacokinetics of Polymeric Nanoparticles. *Int. J. Pharm.* **2006**, *307*, 93–102.

11. Schiffelers, R. M.; Ansari, A.; Xu, J.; Zhou, Q.; Tang, Q. Q.; Storm, G.; Molema, G.; Lu, P. Y.; Scaria, P. V.; Woodle, M. C. Cancer SiRNA Therapy by Tumor Selective Delivery with Ligand-Targeted Sterically Stabilized Nanoparticle. *Nucleic Acids Res.* **2004**, *32*, e149.

12. Farokhzad, O. C.; Cheng, J. J.; Teply, B. A.; Sherifi, I.; Jon, S.; Kantoff, P. W.; Richie, J. P.; Langer, R. Targeted Nanoparticle—Aptamer Bioconjugates for Cancer Chemotherapy *In Vivo*. *Proc. Natl. Acad. Sci. U.S.A.* **2006**, *103*, 6315–6320.

13. Bartlett, D. W.; Su, H.; Hildebrandt, I. J.; Weber, W. A.; Davis, M. E. Impact of Tumor-Specific Targeting on the Biodistribution and Efficacy of SiRNA Nanoparticles Measured by Multimodality *In Vivo* Imaging. *Proc. Natl. Acad. Sci. U.S.A.* **2007**, *104*, 15549–15554.

14. Kirpotin, D. B.; Drummond, D. C.; Shao, Y.; Shalaby, M. R.; Hong, K. L.; Nielsen, U. B.; Marks, J. D.; Benz, C. C.; Park, J. W. Antibody Targeting of Long-Circulating Lipidic Nanoparticles Does Not Increase Tumor Localization but Does Increase Internalization in Animal Models. *Cancer Res.* **2006**, *66*, 6732–6740.

15. Corsten, M. F.; Shah, K. Therapeutic Stem-Cells for Cancer Treatment: Hopes and Hurdles in Tactical Warfare. *Lancet Oncol.* **2008**, *9*, 376–384.

16. Studeny, M.; Marini, F. C.; Champlin, R. E.; Zompetta, C.; Fidler, I. J.; Andreeff, M. Bone Marrow-Derived Mesenchymal Stem Cells as Vehicles for Interferon-β Delivery into Tumors. *Cancer Res.* **2002**, *62*, 3603–3608.

17. Karnoub, A. E.; Dash, A. B.; Vo, A. P.; Sullivan, A.; Brooks, M. W.; Bell, G. W.; Richardson, A. L.; Polyak, K.; Tubo, R.; Weinberg, R. A. Mesenchymal Stem Cells within Tumour Stroma Promote Breast Cancer Metastasis. *Nature* **2007**, *449*, 557–563.

18. Kidd, S.; Spaeth, E.; Klopp, A.; Andreeff, M.; Hall, B.; Marini, F. C. The (in) Auspicious Role of Mesenchymal Stromal Cells in Cancer: Be It Friend or Foe. *Cytotherapy* **2008**, *10*, 657–667.

19. Nakamizo, A.; Marini, F.; Amano, T.; Khan, A.; Studeny, M.; Gumin, J.; Chen, J.; Hentschel, S.; Vecil, G.; Dembinski, J.; Andreeff, M.; Lang, F. F. Human Bone Marrow-Derived Mesenchymal Stem Cells in the Treatment of Gliomas. *Cancer Res.* **2005**, *65*, 3307–3318.

20. Aboody, K. S.; Najbauer, J.; Schmidt, N. O.; Yang, W.; Wu, J. K.; Zhuge, Y.; Przylecki, W.; Carroll, R.; Black, P. M.; Perides, G. Targeting of Melanoma Brain Metastases Using Engineered Neural Stem/Progenitor Cells. *Neuro-Oncology* **2006**, *8*, 119–126.

21. Choi, M. R.; Stanton-Maxey, K. J.; Stanley, J. K.; Levin, C. S.; Bardhan, R.; Akin, D.; Badve, S.; Sturgis, J.; Robinson, J. P.; Bashir, R.; Halas, N. J.; Clare, S. E. A Cellular Trojan Horse for Delivery of Therapeutic Nanoparticles into Tumors. *Nano Lett.* **2007**, *7*, 3759–3765.

22. Swiston, A. J.; Cheng, C.; Um, S. H.; Irvine, D. J.; Cohen, R. E.; Rubner, M. F. Surface Functionalization of Living Cells with Multilayer Patches. *Nano Lett.* **2008**, *8*, 4446–4453.

23. Chambers, E.; Mitragotri, S. Long Circulating Nanoparticles *via* Adhesion on Red Blood Cells: Mechanism and Extended Circulation. *Exp. Biol. Med.* **2007**, *232*, 958–966.

24. Chithrani, B. D.; Ghazani, A. A.; Chan, W. C. W. Determining the Size and Shape Dependence of Gold Nanoparticle Uptake into Mammalian Cells. *Nano Lett.* **2006**, *6*, 662–668.

25. Caswell, P.; Norman, J. Endocytic Transport of Integrins during Cell Migration and Invasion. *Trends Cell Biol.* **2008**, *18*, 257–263.

26. Lauffenburger, D. A.; Horwitz, A. F. Cell Migration: A Physically Integrated Molecular Process. *Cell* **1996**, *84*, 359–369.

27. Ridley, A. J.; Schwartz, M. A.; Burridge, K.; Firtel, R. A.; Ginsberg, M. H.; Borisy, G.; Parsons, J. T.; Horwitz, A. R. Cell Migration: Integrating Signals from Front to Back. *Science* **2003**, *302*, 1704–1709.

28. Gao, H. J.; Shi, W. D.; Freund, L. B. Mechanics of Receptor-Mediated Endocytosis. *Proc. Natl. Acad. Sci. U.S.A.* **2005**, *102*, 9469–9474.

29. Jin, H.; Heller, D. A.; Sharma, R.; Strano, M. S. Size-Dependent Cellular Uptake and Expulsion of Single-Walled Carbon Nanotubes: Single Particle Tracking and a Generic Uptake Model for Nanoparticles. *ACS Nano* **2009**, *3*, 149–158.

30. Sasportas, L. S.; Kasmieh, R.; Wakimoto, H.; Hingtgen, S.; van de Water, J.; Mohapatra, G.; Figueiredo, J. L.; Martuza, R. L.; Weissleder, R.; Shah, K. Assessment of Therapeutic Efficacy and Fate of Engineered Human Mesenchymal Stem Cells for Cancer Therapy. *Proc. Natl. Acad. Sci. U.S.A.* **2009**, *106*, 4822–4827.

31. Sipkins, D. A.; Wei, X. B.; Wu, J. W.; Runnels, J. M.; Cote, D.; Means, T. K.; Luster, A. D.; Scadden, D. T.; Lin, C. P. *In Vivo* Imaging of Specialized Bone Marrow Endothelial Microdomains for Tumour Engraftment. *Nature* **2005**, *435*, 969–973.

32. Sackstein, R.; Merzaban, J. S.; Cain, D. W.; Dagia, N. M.; Spencer, J. A.; Lin, C. P.; Wohlgemuth, R. *Ex Vivo* Glycan Engineering of Cd44 Programs Human Multipotent Mesenchymal Stromal Cell Trafficking to Bone. *Nat. Med.* **2008**, *14*, 181–187.

33. Ponte, A. L.; Marais, E.; Gallay, N.; Langonne, A.; Delorme, B.; Herault, O.; Charbord, P.; Domenech, J. The *In Vitro* Migration Capacity of Human Bone Marrow Mesenchymal Stem Cells: Comparison of Chemokine and Growth Factor Chemotactic Activities. *Stem Cells* **2007**, *25*, 1737–1745.

34. Klopp, A. H.; Spaeth, E. L.; Dembinski, J. L.; Woodward, W. A.; Munshi, A.; Meyn, R. E.; Cox, J. D.; Andreeff, M.; Marini, F. C. Tumor Irradiation Increases the Recruitment of Circulating Mesenchymal Stem Cells into the Tumor Microenvironment. *Cancer Res.* **2007**, *67*, 11687–11695.

35. Conner, S. D.; Schmid, S. L. Regulated Portals of Entry into the Cell. *Nature* **2003**, *422*, 37–44.